Gas-Phase Reaction of Monomethylhydrazine with Ozone: Kinetics and OH Radical Formation

S. RICHTERS, T. BERNDT

Leibniz-Institut für Troposphärenforschung e.V., Permoserstr. 15, 04318, Leipzig, Germany

Received 8 April 2013; revised 26 July 2013; accepted 29 July 2013

DOI 10.1002/kin.20816

ABSTRACT: The gas-phase reaction of monomethylhydrazine ($CH_3NH–NH_2$; MMH) with ozone was investigated in a flow tube at atmospheric pressure and a temperature of 295 ± 2 K using N_2/O_2 mixtures (3–30 vol% O_2) as the carrier gas. Proton transfer reaction–mass spectrometry (PTR-MS) and long-path FT-IR spectroscopy served as the main analytical techniques. The kinetics of the title reaction was investigated with a relative rate technique yielding $k_{MMH+O3} = (4.3 \pm 1.0) \times 10^{-15}$ cm^3 molecule^{-1} s^{-1}. Methyldiazene ($CH_3N{=}NH$; MeDia) has been identified as the main product in this reaction system as a result of PTR-MS analysis. The reactivity of MeDia toward ozone was estimated relative to the reaction of MMH with ozone resulting in $k_{MeDia+O3} = (2.7 \pm 1.6) \times 10^{-15}$ cm^3 molecule^{-1} s^{-1}. OH radicals were followed indirectly by phenol formation from the reaction of OH radicals with benzene. Increasing OH radical yields with increasing MMH conversion have been observed pointing to the importance of secondary processes for OH radical generation. Generally, the detected OH radical yields were definitely smaller than thought so far. The results of this study do not support the mechanism of OH radical formation from the reaction of MMH with ozone as proposed in the literature. © 2013 Wiley Periodicals, Inc. Int J Chem Kinet 46: 1–9, 2014

INTRODUCTION

The OH radical is the most important oxidant in the atmosphere beside ozone, NO_3 radicals, and Cl atoms. Reliable OH radical sources are needed in laboratory experiments investigating atmospheric oxidation processes. Mostly used approaches are photolysis of HONO [1], H_2O_2 [2], O_3 [3] or CH_3ONO [4]. On the other hand, ozonolysis of olefins represents a non-photolytic OH radical source also applicable for low-NO_x studies [5]. This path of OH radical generation, however, is inevitably associated with the formation of a series of organic oxidation products arising from the ozonolysis itself and the unwanted, consecutive reaction of the olefins (used for ozonolysis) with OH radicals.

A possible application of the reaction of hydrazine or methyl-substituted hydrazines with ozone as an OH radical source has been already discussed early in the 1980s [6,7]. Tuazon et al. [6] reported a rate coefficient of the reaction of hydrazine with ozone at 294–297 K, $k_{Hyd + O3} = 1.4 \times 10^{-16}$ cm^3 molecule^{-1} s^{-1}, as a result of a chamber study and concluded that the corresponding rate coefficient for the reaction of monomethylhydrazine ($CH_3NH–NH_2$; MMH) has to be much higher.

Correspondence to: T. Berndt; e-mail: berndt@tropos.de

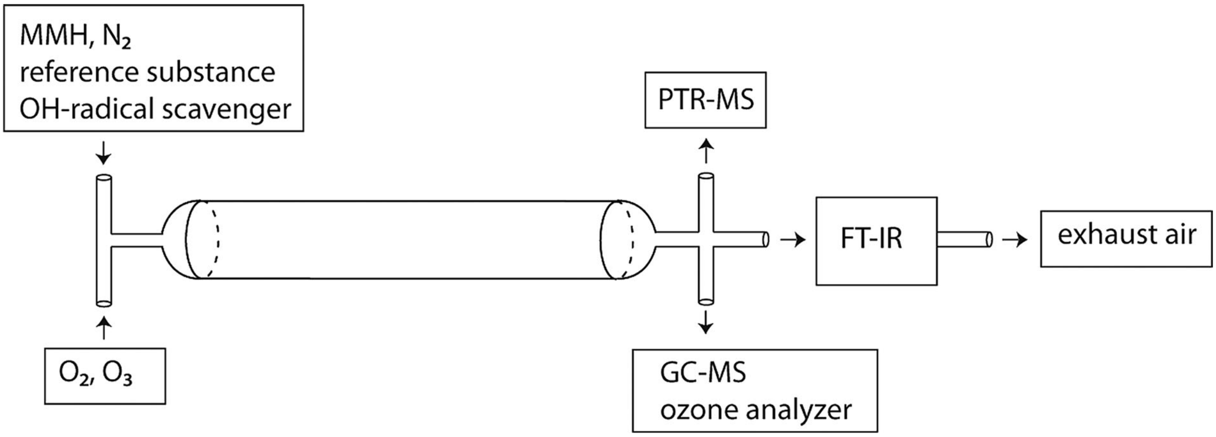

Figure 1 Schematic of the experimental setup.

In contrast to that Martin et al. [8] reported a value of $k_{\mathrm{MMH+O3}} = 8.7 \times 10^{-17}$ cm^3 molecule^{-1} s^{-1} measured at atmospheric pressure in a flow reactor at a temperature of 299 K. It is noteworthy that in this experiment a change of the reaction stoichiometry (reacted [MMH] per reacted [O_3]) was observed starting from unity in the initial stage of the reaction to a value of up to 7 for rising reactant conversions [8]. From a low-pressure flow tube study at room temperature, however, a rate coefficient $k_{\mathrm{MMH+O3}} = 4.5 \times 10^{-14}$ cm^3 molecule^{-1} s^{-1} is reported [9], roughly a factor of 500 higher compared with the work by Martin et al. [8].

The following reaction scheme for the initial step of the reaction of MMH with ozone is proposed in the literature [6,8,9]:

$$CH_3NH-NH_2 + O_3 \rightarrow CH_3NH{-}(N^\bullet)H + OH + O_2 \quad \text{(R1)}$$

$$CH_3NH{-}(N^\bullet)H + O_2 \rightarrow CH_3N=NH + HO_2 \quad \text{(R2)}$$

$$CH_3N=NH + O_3 \rightarrow CH_3N=N^\bullet + OH + O_2 \quad \text{(R3)}$$

First, H-abstraction of a nitrogen-bound H-atom by ozone takes place (R1) followed by an H-abstraction step by O_2 forming methyldiazene ($CH_3N{=}NH$; MeDia) (R2). Furthermore, MeDia can also be attacked by ozone abstracting the remaining nitrogen-bound H-atom with subsequent OH radical formation (R3). The pathways (R1)–(R3) describe efficient HO_x formation. As a result of the possible reaction of OH radicals with MMH and MeDia, secondary products such as diazomethane (CH_2N_2) and formaldehyde can be formed. It is to be noted that OH radical generation has been shown so far only qualitatively [7]. In the literature, there is no determination of the OH radical yield given that confirms the proposed pathways (R1) and (R3).

The aim of this work is to reinvestigate the rate coefficient of the reaction of MMH with ozone to overcome the discrepancy of the kinetics of this step at room temperature conditions. The experimental determination of the OH radical yield should help to assess the title reaction as a potential OH radical source in laboratory investigations.

EXPERIMENTAL

The experiments were performed in an atmospheric pressure flow tube with a length of 150 cm and an inner diameter (i.d.) of 15 cm using O_2/N_2 mixtures (3–20 vol% O_2) as the carrier gas. A total flow was set at 15,000 cm^3 min^{-1} (STP) at 295 ± 2 K leading to a bulk residence time of 106 s (cf. Fig. 1). Ozone was generated by flushing 100 cm^3 min^{-1} (STP) gas (10–100 vol% O_2 with N_2 balance) through an ozone generator (UVP PS-4), further diluted downstream with O_2, and mixed with the main gas stream (N_2, MMH, etc.) in a turbulent gas mixer just before the entrance of the flow tube. The turbulent mixing process ensures homogeneous reactant concentrations at the flow tube entrance. MMH was stored in a flask maintained at 228 K, carried along with 1–20 cm^3 min^{-1} (STP) N_2, and diluted immediately with the main N_2 stream. Further additions, such as OH radical scavengers (CO, C_3H_8, and H_2), the olefins serving as reference substances or C_6H_6, were also added to the main N_2 stream before it was fed into the ozone/O_2 stream in the turbulent gas mixer. The needed gas mixtures of 2,3-dimethyl-2-butene (TME), 2-methyl-2-butene (MeBut), or benzene were prepared in a gas-mixing unit. All flow rates were set by calibrated mass flow controllers (MKS 1259 and 1179). The detection of the gas-phase species was carried out at the outlet of the flow tube by means of long-path FT-IR spectroscopy (Thermo, Nicolet 6700), proton transfer reaction–mass spectrometry (PTR-MS; Ionicon, HS PTR-QMS 500), online GC-MS analysis (Agilent, GC 6890 with MSD 5973; separation column: HP-5MS 19091S-433), and an ozone analyzer (Thermo Fischer, 49C).

For FT-IR spectroscopy, the whole gas stream was pumped continuously through a gas cell equipped with a White mirror system (path length of 20 m). 500–4000 spectra were recorded in the range of 4000–700 cm^{-1} with a resolution of 1 or 8 cm^{-1} using a mercury cadmium telluride detector. The concentration of phenol was determined using the calibrated spectrum of the reference substance measured in this laboratory [10]. MMH was quantified using a cross section of 8.28×10^{-20} cm^2 $\mathrm{molecule}^{-1}$ for the absorption centered at 888 cm^{-1} [8]. The precision of the MMH concentration was especially important for the determination of the OH radical yield. But no error limit of the MMH cross section was given in the original work. Therefore, the reliability of the cross section was tested in experiments with low MMH conversion (<0.3) in the presence of an OH radical scavenger measuring simultaneously the amount of reacted MMH and ozone (1:1 reaction stoichiometry assumed). Thus, an error of 20% had to take into account (see the Results and Discussion section).

In the case of PTR-MS measurements, the gas was sampled from the center flow at the flow tube outlet to a first pump stage by means of an uncoated, deactivated fused silica capillary (0.32 mm i.d.; length 27 cm). A second capillary (PEEK; 0.25 mm i.d.; length 7 cm) connected the first pump stage with the drift tube of the mass spectrometer. The drift tube voltage was set at 500 V, and the raw data were corrected by the instrument's transmission factor. The PTR-MS operated in the multiple ion detection mode (MID) or the scan mode (30–90 amu).

For GC-MS analysis, a small flow was pumped continuously through a heated GC-loop coupled with a prefocusing device where the gas sample from the GC-loop was flushed through an uncoated, deactivated fused silica capillary (0.32 mm i.d.) and trapped at liquid N_2 temperature. After flash heating, the substances were directly injected at the separation column.

Gas sampling for PTR-MS measurements, GC-MS analysis, as well as for ozone monitoring was carried out at the same sampling point.

The initial concentrations were (unit: molecule cm^{-3}) MMH: $(6.6\text{–}132) \times 10^{11}$, ozone: $(4.0\text{–}780) \times 10^{11}$, C_6H_6: $(1.0\text{–}1000) \times 10^{12}$, CO: $(1.6\text{–}3.2) \times 10^{17}$, H_2: 8.2×10^{17}, C_3H_8: 1.6×10^{16}, TME: 4.1×10^{12}, and MeBut: 4.1×10^{12}.

Chemicals

The gases had stated purities as follows: O_2 (99.999%; Air Products, Hattingen, Germany), N_2 (99.9999%; Air Products, further purified with Aeronex gatekeeper gas purifier SS-500K-I-4R), H_2 (99.9992%; Air Products), CO (99.997%; Air Products), C_3H_8 (99.95%; Linde, Pullach, Germany), He (99.9997%; Air Products). MMH (98%; Aldrich, Steinheim, Germany), TME (99.5%; Fluka, Steinheim, Germany), MeBut (95%; Fluka), and C_6H_6 (99.9%; Aldrich) and were used as purchased.

Kinetics

Relative Rate Technique. The relative rate technique was applied for the determination of the rate coefficient of the reaction of MMH with ozone. TME and MeBut served as the reference substances with the corresponding rate coefficients $k_{\mathrm{TME+O3}} = (1.0 \pm 0.2) \times 10^{-15}$ cm^3 $\mathrm{molecule}^{-1}$ s^{-1} and $k_{\mathrm{MeBut+O3}} = (4.1 \pm 0.5) \times 10^{-15}$ cm^3 $\mathrm{molecule}^{-1}$ s^{-1} [11]. (Note: Given pathways (R1), (R1a), and (R1b) are different only in the description of the reaction products, but describing the same reaction with the same rate coefficient k_1.)

$$\mathrm{MMH} + \mathrm{O_3} \rightarrow \mathrm{Products} \tag{R1a}$$

$$\mathrm{Reference} + \mathrm{O_3} \rightarrow \mathrm{Products} \tag{R4}$$

The measurements were carried out by means of the PTR-MS in the MID mode monitoring MMH-H^+ at $m/z = 47$ amu, TME-H^+ at $m/z = 85$ amu, and MeBut-H^+ at $m/z = 71$ amu. These ion traces were not influenced by any product ions as confirmed in preexperiments each.

The relative rate coefficient of the reaction of MMH with O_3 (R1a) regarding the reaction of the reference substance with O_3 (R4), k_1/k_4, was derived according to Eq. (I):

$$\ln \frac{[\mathrm{MMH}]_\mathrm{t}}{[\mathrm{MMH}]_0} = \frac{k_1}{k_4} \ln \frac{[\mathrm{reference}]_\mathrm{t}}{[\mathrm{reference}]_0} \tag{I}$$

The concentrations in the absence of O_3 are expressed with index "0" and in the presence of O_3 with index "t". The consumption of MMH and the reference substance was varied by changing the ozone concentration.

Consecutive Reaction of MeDia with Ozone. A consecutive reaction of MeDia with ozone had to be taken into account due to the measured concentration profiles. This reaction path was already discussed in the literature as a result of former experimental studies [6,8,9]. The following simple reaction scheme is assumed allowing the determination of the rate coefficient ratio k_1/k_3:

$$\mathrm{MMH} + \mathrm{O_3} \rightarrow y_1 \cdot \mathrm{MeDia} + \cdots \qquad \text{(R1b)}$$

$$\mathrm{MeDia} + \mathrm{O_3} \rightarrow \mathrm{Products} \qquad \text{(R3a)}$$

The resulting differential equations (II) and (III) of pathways (1b) and (3a)

$$\frac{\mathrm{d}\,[\mathrm{MMH}]}{\mathrm{d}t} = -k_1\,[\mathrm{O_3}]\,[\mathrm{MMH}] \qquad \text{(II)}$$

$$\frac{\mathrm{d}\,[\mathrm{MeDia}]}{\mathrm{d}t} = y_1 k_1\,[\mathrm{O_3}]\,[\mathrm{MMH}] - k_3\,[\mathrm{O_3}]\,[\mathrm{MeDia}] \qquad \text{(III)}$$

yield after rearrangement of Eq. (IV)

$$\frac{\mathrm{d}[\mathrm{MeDia}]}{\mathrm{d}[\mathrm{MMH}]} = -y_1 + \frac{k_3}{k_1}\frac{[\mathrm{MeDia}]}{[\mathrm{MMH}]} \qquad \text{(IV)}$$

The parameters y_1 and k_3/k_1 were determined using a least-squares analysis for nonlinear parameter estimation by means of a damped Gauss–Newton algorithm based on experimental data for MMH and MeDia. The needed integration of Eq. (IV) was done numerically with the help of a semi-implicit step method [12].

OH Radical Formation

The OH radical generation was followed indirectly investigating the phenol formation from the reaction of OH radicals with benzene being in competition with the reaction of OH radicals with MMH (cf. pathways (R5) and (R6)). The knowledge of the integrated rates x_1, x_5, and x_6 according to the reactions (R1c), (R5), and (R6), respectively, and their rate coefficients k_5 and k_6 allows a rough estimate of the OH radical yield y_2 from reaction (R1c):

$$\mathrm{O_3} + \mathrm{MMH} \rightarrow y_2 \cdot \mathrm{OH} + \cdots \qquad \text{(R1c)}$$

$$\mathrm{OH} + \mathrm{MMH} \rightarrow \mathrm{Products} \qquad \text{(R5)}$$

$$\mathrm{OH} + \mathrm{C_6H_6}\ (+\mathrm{O_2}) \rightarrow 0.61 \cdot \mathrm{C_6H_5OH} + \cdots \qquad \text{(R6)}$$

The needed rate coefficient of reactions (R5) and (R6) were taken from the literature, $k_5 = 6.11 \times 10^{-11}$ cm^3 molecule^{-1} s^{-1} [13] and $k_6 = 1.26 \times 10^{-12}$ cm^3 molecule^{-1} s^{-1} [14]. A phenol formation yield of 0.61 ± 0.07 was applied as reported in the literature [15]. The phenol concentration and the converted MMH were measured either by means of FT-IR spectroscopy or using PTR-MS analysis.

It is to be noted that only OH radical consumption by MMH and benzene has been considered for simplicity. Additional OH radical reactions with MMH products can lead to an underestimation of y_2, especially for conditions of a relatively high MMH conversion. On the other hand, additional OH radical generation via the reaction of the MeDia with ozone can occur resulting in a possible overestimation of y_2. Therefore, the simple approach used here is able to bring out reliable y_2 data only for conditions of low MMH conversion where secondary processes are of less importance.

The integrated rate x_6 is given by the measured phenol concentration due to the selectivity of phenol formation from reaction (R6):

$$x_6 = \frac{1}{0.61}\,[\mathrm{Phenol}]_\mathrm{t} \qquad \text{(V)}$$

The value x_5 is directly derived from x_6 according to the kinetics of the competitive reactions (R5) and (R6):

$$x_5 = \frac{k_5}{k_6}\frac{\overline{[\mathrm{MMH}]}}{[\mathrm{benzene}]}x_6 \qquad \text{(VI)}$$

The benzene concentration is equal to the initial value due to the very low benzene conversion in the course of the reaction. In the case of MMH, an averaged concentration is taken, $\overline{[\mathrm{MMH}]} = [\mathrm{MMH}]_0 - 0.5 \cdot \Delta[\mathrm{MMH}]$. The value $\Delta[\mathrm{MMH}]$ stands for the measured concentration of reacted MMH.

The integrated rate x_1 is found from the material balance for MMH:

$$x_1 = \Delta[\mathrm{MMH}] - x_5 \qquad \text{(VII)}$$

Setting the OH radical formation equal to the loss processes, Eq. (VIII) follows:

$$y_2 = \frac{x_5 + x_6}{x_1} \qquad \text{(VIII)}$$

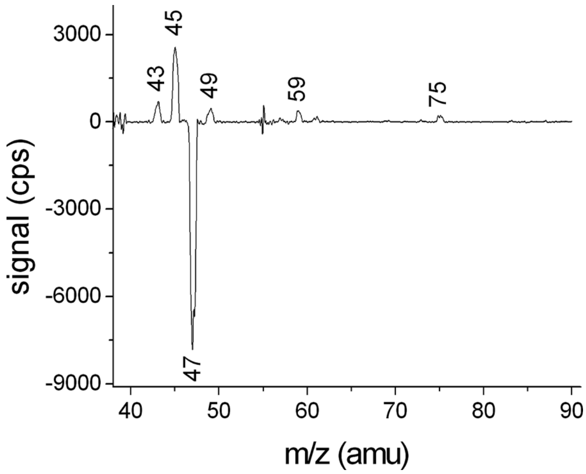

Figure 2 Typical difference spectrum from PTR-MS analysis (ozone production: on/off). Initial concentrations (molecule cm^{-3}): [MMH] = 6.6 × 10^{11}; [O_3] = 5.0 × 10^{12}; [H_2] = 1.6 × 10^{17}; [O_2] = 8.2 × 10^{17}.

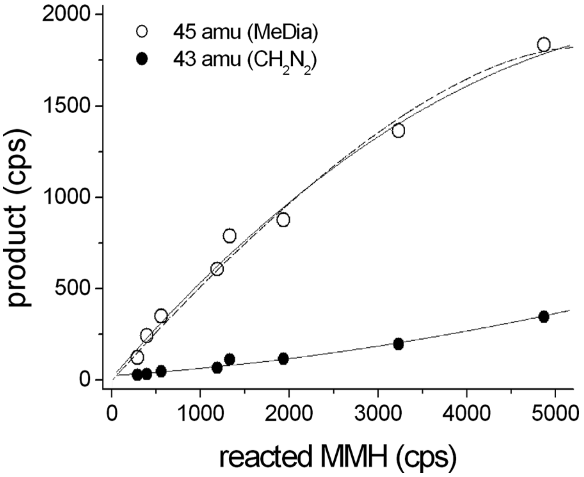

Figure 3 Product formation at 45 amu (MeDia) and 43 amu (CH_2N_2) as a function of reacted MMH, PTR-MS analysis. Initial concentrations (molecule cm^{-3}): [MMH] = 6.6 × 10^{11}; [O_3] = (4.0–250) × 10^{10}; [H_2] = 8.2 × 10^{17}; [O_2] = 8.2 × 10^{17}. The dashed line shows the modeling results according to Eq. (IV).

RESULTS AND DISCUSSION

Product formation

In Fig. 2, a typical PTR-MS difference spectrum (ozone production: on/off) from a reaction in the presence of H_2 as an OH radical scavenger is shown. In this run, ozone was chosen in large excess over MMH resulting in a MMH conversion >0.9. Reacted MMH appears as a negative signal at 47 amu (MMH-H$^+$) and the products as positive signals. The main product at 45 amu was assigned to protonated MeDia. The formation of MeDia is in line with observations from former studies [6,8,9]. The signal at 43 amu was tentatively assigned to protonated diazomethane. This assignment was supported by simultaneously performed FT-IR measurements showing a distinct absorption centered at 2115 cm^{-1}, typical for diazomethane [6]. At the moment, there exists no reasonable explanation regarding the chemical composition of other products responsible for the signals at 49, 59, and 75 amu. In Fig. 3 the product signal strength at 45 amu (MeDia) and 43 amu (CH_2N_2) is depicted as a function of converted MMH from a measurement series in the presence of H_2 for OH radical scavenging. A curvature in the plot of MeDia (45 amu) versus reacted MMH is visible, especially for a relative high MMH conversion. This fact points to a consecutive reaction of MeDia, most probably by ozone (cf. pathway (R3)). On the other hand, the shape of the curve of the signal at 43 amu attributed to CH_2N_2 indicates that this substance is produced in secondary processes, at least partly.

Furthermore, it was tested for possible NO_x formation using NO_2 measurements by means of FT-IR spectroscopy at 1628 cm^{-1}. NO was transformed to NO_2 under the chosen experimental conditions of high ozone concentrations. The found NO_2 concentration was below the detection limit of the FT-IR analysis (5 × 10^9 molecule cm^{-3}) even in experiments with the highest MMH conversion of about 1 × 10^{13} molecule cm^{-3}. A NO_x yield <0.0005 can be inferred from these measurements. It was also tested for possible HCHO formation using FT-IR measurements with a resolution of 1 cm^{-1}. The expected signal centered at 1746 cm^{-1} (a detection limit of about 10^{10} molecule cm^{-3}) was only slightly above the background scattering, and the reproducibility of this signal from one experiment to the next was insufficient. A conservative estimate results in a HCHO yield <0.005.

Kinetics of the Reaction of MMH with Ozone

The relative depletion of MMH (47 amu) and reference substance (here TME at 85 amu) in the reaction with ozone (in the presence of OH radical scavengers) was followed by means of PTR-MS measurements using the MID (cf. Fig. 4). Increasing reactant consumption (MMH and the reference substances) was achieved by increasing ozone concentrations. After switching on the ozone generator, rising ozone production occurs within the warm-up period of 5–10 min providing the desired change of the ozone concentration. The measured data for MMH conversions $\leq$0.6 were taken for

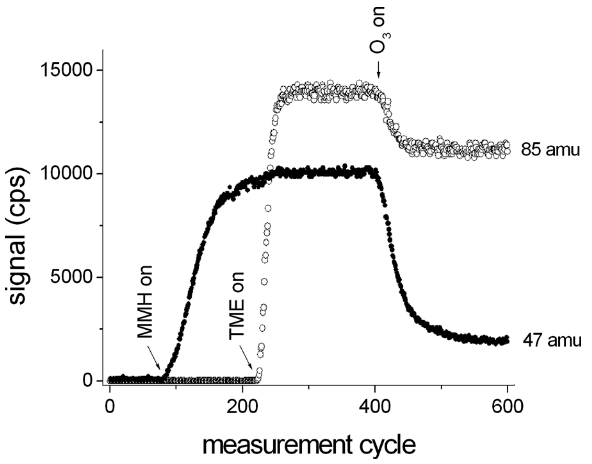

Figure 4 Reaction of MMH (47 amu) and TME (85 amu) with ozone, PTR-MS analysis. Initial concentrations (molecule cm^3): [MMH] = 6.6×10^{11}; $[O_3]_{max} = 2.5 \times 10^{12}$; [TME] = 4.1×10^{12}; [CO] = 1.6×10^{17}; $[O_2] = 8.2 \times 10^{17}$.

the kinetic analysis according to Eq. (I) (see Fig. 5). The experiments were carried out with two reference substances, TME or MeBut, two different OH radical scavengers, C_3H_8 or CO, and for two different O_2 concentrations balances by N_2, 8.2×10^{17} or 4.9×10^{18} molecule cm^{-3}. No significant influence of one of these parameters on the resulting rate coefficient was obtained. The experimental conditions along with the kinetic findings from a linear regression analysis are summarized in Table I. All errors given represent 2σ

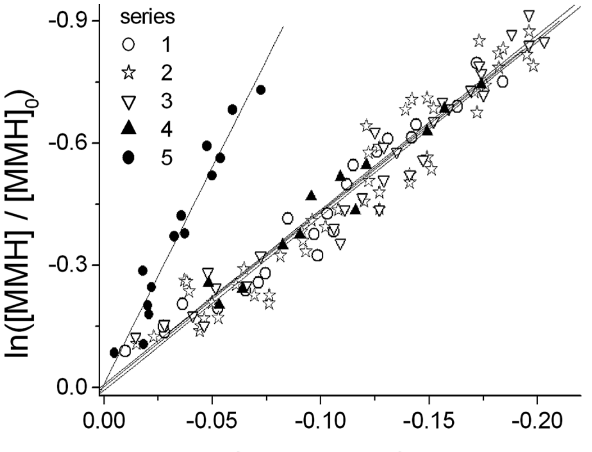

Figure 5 Experimental data for the reaction of MMH with ozone plotted according to Eq. (I). Experimental conditions and the findings are summarized in Table I. The lines represent the individual result from the regression analysis for each measurement series.

Table I Experimental Conditions and the Results of the Kinetic Investigation for the Rate Coefficient of the Reaction of MMH with Ozone, k_1; the Initial MMH Concentration was 6.6×10^{11} Molecule cm^{-3}

Series	$[O_2]$ ($\times 10^{17}$ molecule cm^{-3})	[Reference] ($\times 10^{12}$ molecule cm^{-3})	[OH scavenger] ($\times 10^{16}$ molecule cm^{-3})	k_1/k_4	Intercept	k_1 ($\times 10^{-15}$ cm^3 molecule^{-1} s^{-1})
1	8.2	[TME] = 4.1	$[C_3H_8]$ = 1.6	4.3 ± 0.4	0.003 ± 0.04	4.3 ± 0.9
2	8.2	[TME] = 4.1	[CO] = 16	4.3 ± 0.6	−0.01 ± 0.06	4.3 ± 1.0
3	8.2	[TME] = 4.1	[CO] = 33	4.3 ± 0.4	0.009 ± 0.06	4.3 ± 0.9
4	49	[TME] = 4.1	[CO] = 16	4.3 ± 0.6	0.009 ± 0.06	4.3 ± 1.0
5	8.2	[MeBut] = 4.1	[CO] = 16	10.3 ± 1.6	−0.01 ± 0.06	4.2 ± 0.8
Mean						4.3 ± 1.0

limits. In the case of the rate coefficient k_1, the propagation of error includes the experimental error of k_1/k_4 and the error of the rate coefficient of the reference reaction.

As a result of this study, a rate coefficient $k_{\mathrm{MMH+O3}} = (4.3 \pm 1.0) \times 10^{-15}$ cm^3 molecule^{-1} s^{-1} at 295 ± 2 K can be given. This value is qualitatively in line with the finding by Tuazon et al. [6] stating a rate coefficient for $k_{\mathrm{MMH+O3}}$ to be much higher than 1.4×10^{-16} cm^3 molecule^{-1} s^{-1}. However, our value is neither in a reasonable agreement with the data by Martin et al. ($k_{\mathrm{MMH+O3}} = 8.7 \times 10^{-17}$ cm^3 molecule^{-1} s^{-1}) [8] nor with that by Coleman et al. ($k_{\mathrm{MMH+O3}} = 4.5 \times 10^{-14}$ cm^3 molecule^{-1} s^{-1}) [9]. An explanation for this distinct disagreement of our value with both literature data cannot be specified.

Kinetics of the Consecutive Reaction of MeDia with Ozone

The product analysis revealed that the formed MeDia undergoes a consecutive reaction most likely with ozone (in the presence of an OH radical scavenger) (cf. Fig. 3. This pathway was already proposed in the literature [6,8,9]. The rate coefficient of the reaction of MeDia with ozone, k_3, was estimated relative to k_1 based on the MeDia measurements as a function of reacted MMH as given in Fig. 3, [MMH] = 6.6×10^{11}; [H_2] = 8.2×10^{17}; [O_3] = $(4.0\text{–}250) \times 10^{10}$ molecule cm^{-3}. It was assumed that the signal measured at 45 amu from the PTR-MS analysis was exclusively due to MeDia. According to reactions (R1b) and (R3a), the differential equation (IV) follows. Equation (IV) was integrated numerically. Supposing first of all that the efficiency of PTR-MS detection for MMH and MeDia is equal (i.e., the same rate coefficients of protonaton, $k(\mathrm{MMH} + H_3O^+)/k(\mathrm{MeDia} + H_3O^+) = 1$), the measured signals of MMH and MeDia can be used for the nonlinear parameter estimation without any correction factor. The initial values of MMH and MeDia needed for integration are set at 7450 and 0 cps, respectively, according to the measured signal strengths at 47 and 45 amu without ozone addition. The nonlinear parameter estimation yielded $y_1 = 0.54 \pm 0.04$ and $k_3/k_1 = 0.63 \pm 0.34$. The dashed line in Fig. 3 represents the result of the fitting procedure. A sensitivity study showed that the obtained ratio k_3/k_1 was independent of the assumed PTR-MS detection efficiency for MMH and MeDia. The parameter y_1 (MeDia yield from reaction (R1b)), however, showed a clear dependence on this assumption. Table II summarizes the results of the sensitivity study assuming $k(\mathrm{MMH} + H_3O^+)/k(\mathrm{MeDia} + H_3O^+) = 0.5$ or 2. Using our value $k_1 = (4.3 \pm 1.0) \times 10^{-15}$ cm^3 molecule^{-1} s^{-1}, a rate coefficient for the reaction of MeDia with ozone $k_3 = (2.7 \pm 1.6) \times 10^{-15}$ cm^3 molecule^{-1} s^{-1} follows. The given error includes the uncertainty of k_3/k_1 and the error of the rate coefficient of the reference reaction (2σ limits).

Table II Results of the Sensitivity Study Investigating the Effect of the PTR-MS Detection Efficiency for MMH and MeDia on the Parameters k_3/k_1 and the Yield y_1

$k(\mathrm{MMH} + H_3O^+)/$ $k(\mathrm{MeDia} + H_3O^+)$	k_3/k_1	y_1
0.5	0.63 ± 0.34	0.27 ± 0.02
1.0	0.63 ± 0.34	0.54 ± 0.04
2.0	0.63 ± 0.34	1.07 ± 0.09

Martin et al. [8] reported a rate coefficient for the reaction of MeDia with ozone $k_{\mathrm{MeDia+O3}} = (2.5 \pm 0.1) \times 10^{-16}$ cm^3 molecule^{-1} s^{-1} about one order of magnitude lower than our value. Also here, no reasoned explanation for the discrepancy can be given.

OH Radical Formation

Formed OH radicals from the reaction of MMH with ozone were detected indirectly using phenol formation from the reaction of OH radicals with benzene. Measurements with all analytical techniques (GC-MS, PTR-MS, FT-IR) confirmed the formation of phenol in a wide range of reactant concentrations; [MMH] = 6.6×10^{11} and [C_6H_6] = 5.0×10^{12} molecule cm^{-3} used for PTR-MS and GC-MS analysis; [MMH] = 1.3×10^{13} and [C_6H_6] = 1.1×10^{15} molecule cm^{-3} used for FT-IR and GC-MS analysis. The O_2 concentration was set at 8.2×10^{17} or 8.2×10^{18} molecule cm^{-3}, and ozone was varied to achieve different MMH conversions.

The diffusion-controlled wall loss of OH radicals was estimated considering the first-order rate law with $k_{\mathrm{wall}} = 3.65 \cdot D/r^2 = 0.014$ s^{-1} using $D = 0.22$ cm^2 s^{-1} [16]. Even for the lowest benzene concentration of 5.0×10^{12} molecule cm^{-3}, $k_6 \cdot [C_6H_6] = 6.3$ s^{-1} follows making the wall loss of OH radicals negligible under all conditions.

For instance, Fig. 6 shows results from FT-IR measurements comparing the detected reaction products from runs in the presence (a, b) and the absence (c) of benzene. Phenol formation has been identified by its absorptions at 1607 and 3652 cm^{-1} (a). After phenol subtraction using a reference spectrum, there was remaining product absorption at 1714 cm^{-1} arising from benzene oxidation (b). This signal is very likely due to unsaturated carbonyls, known products of benzene oxidation beside phenol [10]. No effort was undertaken in

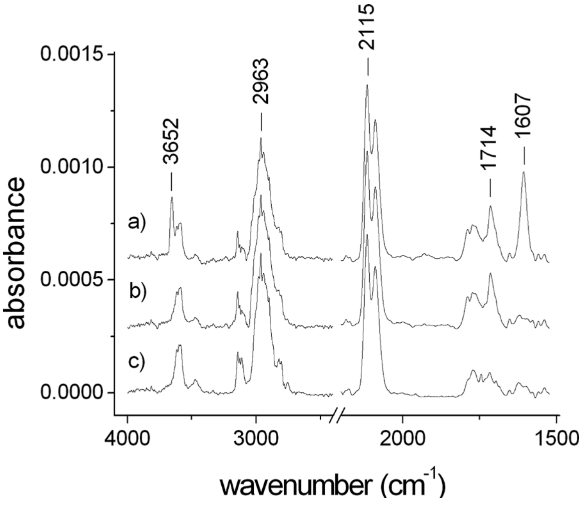

Figure 6 FT-IR spectra (resolution: 8 cm^{-1}, 2000 scans) of the products from the reaction of MMH with ozone, residual reactants have been subtracted: (a) and (b) Product formation in the presence of benzene; in (b) absorptions from phenol are subtracted. (c) Product formation in the absence of benzene. Absorptions at 1607 and 3652 cm^{-1} are due to phenol, at 1714 cm^{-1} from an unsaturated carbonyl of the benzene oxidation, at 2115 cm^{-1} assigned to CH_2N_2, and at 2963 cm^{-1} from a MMH oxidation product not specified. Initial concentrations (molecule cm^{-3}): $[MMH]_0 = 1.3 \times 10^{13}$, $[O_3]_0 = 7.8 \times 10^{12}$, and $[benzene]_0 = 1.1 \times 10^{15}$.

the present study to identify the carbonylic substances formed from benzene.

An attempt was undertaken to quantify the OH radical production in this system. Within a simple reaction scheme, pathways (R1c), (R5), and (R6), the OH radical formation yield from the reaction of MMH with ozone was estimated with the help of Eqs. (V)–(VIII). FT-IR analysis (high reactant concentrations) and PTR-MS measurements (low concentration) were applied to obtain the needed concentrations of phenol and converted MMH. For FT-IR analysis, a calibrated phenol spectrum from our laboratory was used and for the determination of the MMH concentration a cross section of 8.28×10^{-20} cm^2 molecule^{-1} for the absorption at 888 cm^{-1} as given in the literature [8]. In the case of PTR-MS measurements, the MMH-H$^+$ signal at 47 amu was calibrated against simultaneously performed FT-IR measurements at 888 cm^{-1} for elevated MMH concentrations. The C_6H_5OH-H$^+$ signal at 95 amu was calibrated against the 79 amu signal of a well-defined benzene concentration with respect to the different protonation rate coefficients $k(C_6H_5OH + H_3O^+)/k(C_6H_6 + H_3O^+) = 1.26$ [17]. It is to be noted that our determination of the MMH concentration is merely based on a single cross section from the literature [8]. To evaluate the precision of the absolute MMH concentration, the initial reaction stoichiometry (reacted [O_3] per reacted [MMH]) for low MMH conversion (smaller than 0.3) was measured yielding $\Delta[O_3]/\Delta[MMH] = 0.85 \pm 0.08$. This points to an error of the MMH determination of <20% assuming that the deviation from the expected value of unity was mainly due to uncertainties of the MMH concentrations. An error of the MMH concentration of 20% has been taken into account for the calculation of the OH radical yield. The ratio $\Delta[O_3]/\Delta[MMH]$ increased significantly for higher MMH conversions obviously according to secondary processes consuming additional ozone (consecutive MeDia reaction, etc.).

In Fig. 7, the findings for the OH radical yield as a function of converted MMH are depicted. In the error bars, the uncertainties of the concentration determination and the errors of the rate coefficients needed in the calculation are considered. The obtained OH radical yields are substantially lower than the expected yield of unity as given in the literature according to reaction (R1). Moreover, the increase in the OH radical yield with increasing MMH conversion indicates the importance of secondary processes for OH radical formation rather than substantial OH radical production from the reaction of MMH with ozone (R1). The shape of the OH radical yield as a function of reacted MMH in Fig. 7 is similar to the shape of the curve describing the MeDia production as given in Fig. 3. But the used approach (Eqs. (V)–(VIII)) is strictly speaking only valid for low MMH conversions (see the Experimental section), i.e., negligible importance of secondary processes. So we cannot draw any reliable conclusion regarding the OH radical yield from the reaction of MMH with ozone (R1). It could be speculated from

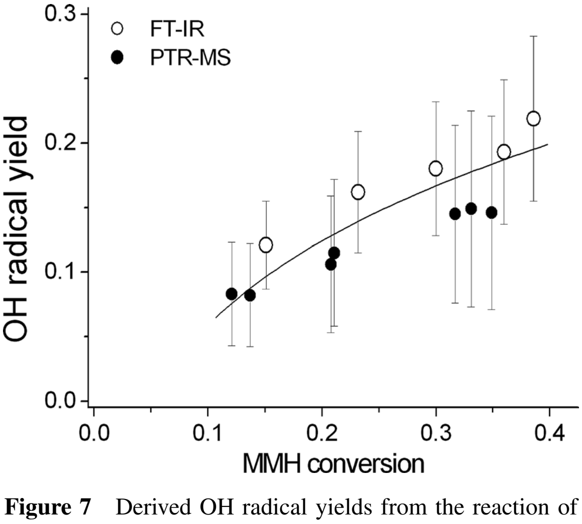

Figure 7 Derived OH radical yields from the reaction of MMH with ozone according to a simplified reaction scheme, pathways (R1c), (R5), and (R6).

our experiments that the OH radical yield from (R1) is very low or close to zero. Nevertheless, OH radicals are clearly formed in the overall process, but especially by secondary processes.

CONCLUSIONS

The gas-phase reaction of MMH with ozone has been studied in a flow tube at atmospheric pressure and a temperature of 295 ± 2 K. MeDia was identified as the main product as a result of the PTR-MS analysis. The kinetics of the reaction of MMH with ozone was investigated with a relative rate technique yielding $k_{\mathrm{MMH+O3}} = (4.3 \pm 1.0) \times 10^{-15}$ cm^3 molecule^{-1} s^{-1}. The rate coefficient of the consecutive reaction of MeDia with ozone was estimated relative to the reaction of MMH with ozone resulting in $k_{\mathrm{MeDia+O3}} = (2.7 \pm 1.6) \times 10^{-15}$ cm^3 molecule^{-1} s^{-1}. OH radicals were measured indirectly by following the phenol formation from the reaction of OH radicals with benzene. Measured OH radical yields were substantially lower than expected from the pathway describing OH radical generation from MMH + O_3 with a yield of unity (R1) as given in the literature. The observed increase in the OH radical yield with increasing MMH conversion points rather to the importance of secondary processes for OH radical generation.

NO_x formation was below the detection limit of the FT-IR analysis, yielding a NO_x yield <0.0005 for the highest MMH conversion of about 1×10^{13} molecule cm^{-3}. There was no clear FT-IR spectroscopic evidence for the production of HCHO (an imaginable product of the methyl group). The HCHO signal from FT-IR measurements was only slightly above the background scattering, and the reproducibility from one experiment to the next was poor. A conservative estimate results in a HCHO yield <0.005.

Although the reaction of MMH with ozone is a less efficient OH radical source than thought, it represents a useful nonphotolytic way of OH radical production for low-NO_x experiments. First experiments in our laboratory regarding the OH radical–initiated oxidation of isoprene under low-NO_x conditions were promising.

The authors thank R. Graefe, K. Pielok, and A. Rohmer for technical assistance.

BIBLIOGRAPHY

1. Niki, H.; Maker, P. D.; Savage, C. M.; Breitenbach, L. P. J Phys Chem 1978, 82, 132.
2. Ohta, T. J Phys Chem 1983, 87, 1209.
3. Robertson, R.; Smith, G. P. J Phys Chem A 2006, 110, 6673.
4. Atkinson, R.; Aschmann, S. M.; Winer, A. M.; Pitts, J. N. Int J Chem Kinet 1982, 14, 507.
5. Siese, M.; Becker, K. H.; Brockmann, K. J.; Geiger, H.; Hofzumahaus, A.; Holland, F.; Mihelcic, D.; Wirtz, K. Environ Sci Technol 2001, 35, 4660.
6. Tuazon, E. C.; Carter, W. P. L.; Winer, A. M.; Pitts, J. N. Environ Sci Technol 1981, 15, 823.
7. Tuazon, E. C.; Carter, W. P. L.; Atkinson, R.; Pitts, J. N. Int J Chem Kinet 1983, 15, 619.
8. Martin, N. B.; Davis, D. D.; Kilduff, J. E.; Mahone, W. C. Final Report, ESL-TR-89–32, Air Force Engineering and Services Center, Tyndall Air Force Base, Bay County, near Panama City, FL, 1989.
9. Coleman, D. J.; Judeikis, H. S.; Lang, V. Final Report, AL/EQ-TR-1993–0029, Air Force Material Command, Tyndall Air Force Base, Bay County, near Panama City, FL, 1996.
10. Berndt, T.; Böge, O. Phys Chem Chem Phys 2001, 3, 4946.
11. Witter, M.; Berndt, T.; Böge, O.; Stratmann, F.; Heintzenberg, J. Int J Chem Kinet 2002, 34, 394.
12. Stoer, J.; Bulirsch, R. Einführung in die Numerische Mathematik II; Springer-Verlag: Berlin, 1987 (in German).
13. Vaghjiani, G. L. Int J Chem Kinet 2001, 33, 354.
14. Atkinson, R. Chem Rev 1986, 86, 69.
15. Berndt, T.; Böge, O. Phys Chem Chem Phys 2006, 8, 1205.
16. Ivanov, A. V.; Trakhtenberg, S.; Bertram, A. K.; Gershenzon, Y. M.; Molina, M. J. J Phys Chem A 2007, 111, 1632.
17. Ionicon, HS. PTR-MS Manual; Ionicon Analytic, 2010.